Extended Abstracts of the 2015 International Conference on Solid State Devices and Materials, Sapporo, 2015, pp882-883

Miniband Formulation in Ge/Si Quantum Dot Array

Yi-Chia Tsai[1], Ming-Yi Lee[2], Yiming Li[1,2,4,*], and Seiji Samukawa[3,4]

[1] Department of Electrical and Computer Engineering, National Chiao Tung University, Hsinchu 300, Taiwan
[2] Institute of Communications Engineering, National Chiao Tung University, Hsinchu 300, Taiwan
[3] Institute of Fluid Science, Tohoku University, Aoba-ku, Sendai, Miyagi 9808577, Japan
[4] WPI-Advanced Institute for Materials Research, Tohoku University, Aoba-ku, Sendai, Miyagi 9808577, Japan
[*]Phone: +886-3-5712121 ext. 52974; e-mail: ymli@faculty.nctu.edu.tw

Abstract

A new 3D simulation technique is advanced to calculate the miniband structure and density of state for well-aligned Ge/Si QDs array. Based on the Bloch theorem and the symmetry of configuration, this method surmounts approximations of Kronig-Penny model with constrain of QDs structure. We intensively explore the coupling and interaction of electronic structures among Ge/Si QDs with various density, size and shape of QDs.

1. Introduction

A prospective candidate among the next-generation high efficiency photovoltaic technologies is the use of semiconductor quantum dots (QDs) [1]. The well-aligned QDs play a crucial role in determining the electronic band structure. For close-packed and well-ordered QDs superlattice, QDs couples with neighboring QDs to broaden the discrete energy levels to form finite-width miniband. With the great development of nano-device processes, a 3D finite element method without constraining on QDs structure is needed and has been proposed to simulate miniband structure and density of state (DoS) [2]. In this work, the dependence of electronic structure on the density, size and shape of Ge/Si QDs array is systematically studied in further to instruct realistic QDs design for photonic device applications.

2. Top-Down Fabrication and Computational Model

By combining the self-assemble bio-template and damage-free neutral beam etching, a top-down process, illustrated in Fig. 1(a), is used to fabricate sub-10-nm uniform and well-aligned type-II Ge/Si QDs superlattice [3]. The etched Ge nanopillar before regrowth matrix in Fig. 1(b) exhibits a good uniformity and alignment. This nanofabrication technique, which controls the QD's thickness by the deposition thickness and its diameter by the bio-template, brings the higher flexibility on engineering quantum levels. As listed in Eq. (1), the electronic structure is numerically solved under the Bloch theorem. First, a unit cell formed by the primitive vectors is defined. Then, based on the symmetry of superlattice, the k-points space is defined in an IBZ. Finally, to get band structure $E_{n,k}$ and Bloch function $u_k(\boldsymbol{r})$, Eq. (1) is discretized within a unit cell in real space and solved by a 3D finite element method solver for each sampling k-point in the irreducible Brillouin zone (IBZ).

3. Results and Discussion

Figure 2 shows the energy distribution in IBZ for the ground band of three different QDs shapes. The energy for the ground band is distributed isotropically in k-space and minimum at Γ point. The spread of ground band energy become smaller because of the decrease in the volume of QD when shape change from disk to cone.

Based on the energy distribution in IBZ, the DoS is calculated numerically using an improved triangle method [5] by Eq. (2). Figure 3 shows the DoS for ellipsoid-shaped QDs superlattice with varied interdot space from 0.3 to 3.3 nm. As the interdot space decreasing, i.e. QDs density increasing, QDs interaction between discrete levels increases and miniband crossing phenomenon occurs especially for higher excited states. Because the highest excited states are mixed and become continuous to Si barrier, the effective bandgap of bulk Si is reduced.

To study the effect of quantum confinement in the z-direction, without loss of generality, as shown in Fig. 4, with varied thickness from 2 to 8 nm, the weaker quantum confinement in the *z*-direction causes the energy level of the ground band to be lower. Meantime, the thickness less affects the bandwidth because the coupling between QDs is strongly related to the distance between QDs in the *x*-*y* plane. The first non-degenerate p-orbit along the *z*-direction, as shown in Fig. 5(a), indicates strong dependence of confinement on QDs thickness and becomes the first excited band for the QDs' thickness 8 nm, as shown in Fig. 5(b). As a consequence of the weaker confinement and larger distance between QDs in the *x*-*y* plane for larger QDs radius, the energy level goes lower and bandwidth goes smaller, as shown in Fig. 6.

Figure 7 functions the trend of the calculated energy levels, bandwidth of ground band with the QDs volume for three different QDs shapes under the same base radius (3 nm). Bigger the QDs volume, lower the energy level and larger the bandwidth. The most sensitive to the QDs volume is the disk-shaped and the least is the cone-shaped. This phenomenon is due to the stronger *z*-confinement and interaction in the *x*-*y* plane for disk-shaped QDs than that for the other shapes.

4. Conclusions

In summary, the dependence on the density, size and shape of Ge/Si QDs array has been reported. The QDs size relates to the number of minibands, while the QDs density has great impact on the QDs interaction and miniband width. Additionally, QDs volume and shape affect the quantum confinement through the geometric symmetry. The energy of disk-shaped QDs is more sensitive to volume among three shapes of QDs. We are currently verifying the results by comparing with measured data.

Acknowledgements

This work was supported in part by the Ministry of Science and Technology of Taiwan under Contract MOST-103-2221-E-009-180.

References

[1] W. Hu et al., in: Tech. Dig. IEDM 2012, pp. 115-118.
[2] M.-Y. Lee et al., IEEE Trans. Electron Devices, under review.
[3] W. Hu et al., J. Appl. Phys., vol. 114, p. 124509, 2013.
[4] M. Igarashi et al., Appl. Phys. Lett., vol. 101, p. 063121, 2012.
[5] J.-H. Lee et al., Phys. Rev. B, vol. 66, p. 233102, 2002.

$$\nabla\left[-\frac{\hbar}{2m^*}\nabla u_k(\boldsymbol{r})\right]-\frac{i\hbar}{m^*}\boldsymbol{k}\cdot\nabla u_k(\boldsymbol{r})+\left[V(\boldsymbol{r})+\frac{\hbar k^2}{2m^*}\right]u_k(\boldsymbol{r})=E_{n,k}u_k(\boldsymbol{r}) \quad (1)$$

$$g(E)=\frac{2}{(2\pi)^2}\int_{\mathrm{BZ}}\frac{dl_E}{|\nabla_k E_{n,k}|}=\frac{2}{(2\pi)^2}\sum_{n,l}\frac{l_n(E,\boldsymbol{k}_l)}{|\nabla_k E_n(\boldsymbol{k}_l)|} \quad (2)$$

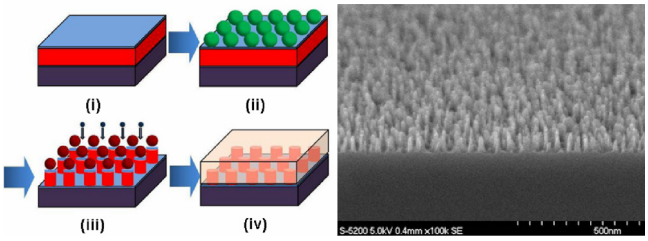

Fig. 1. An advanced top-down nano-fabrication technology [4]. (a) Schematic process flow by (i) Ge/Si stacked layers deposition; (ii) a 2D array ferritin selfassembly and protein shell removal; (iii) damage-free neutral beam etching; (iv) matrix regrowth. (b) SEM image of Ge nanopillars before regrowth matrix for advanced top-down nano-fabrication technology.

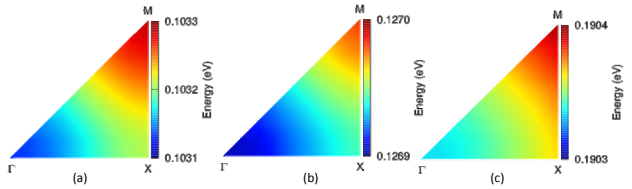

Fig. 2. The energy distribution in IBZ of the ground bounded energy band $E_{0,k}$ for (a) disk-shaped, (b) ellipsoid-shaped and (c) cone-shaped QDs.

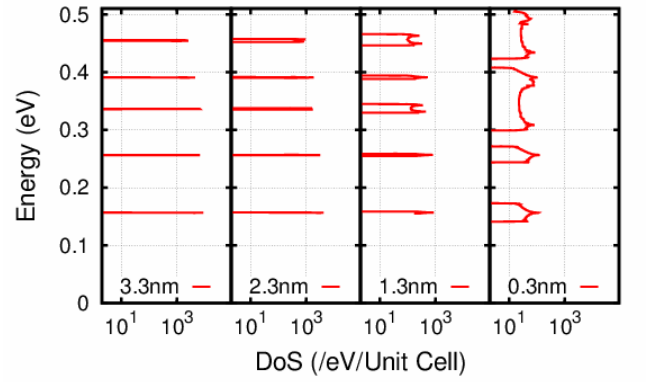

Fig. 3. The density of states for Ge/Si ellipsoid-shaped QDs square superlattice with QD's radius of 2 nm, thickness of 6 nm, and varied interdot space from 3.3 to 0.3 nm.

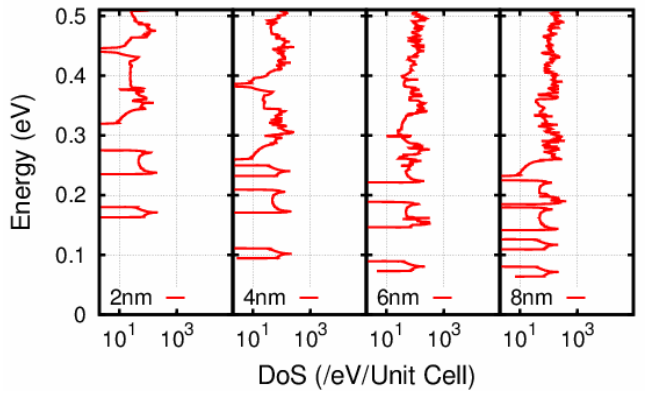

Fig. 4. The density of states for Ge/Si disk-shaped QDs square superlattice with QD radius of 3 nm, interdot space of 0.3 nm, and varied thickness from 2 to 8 nm

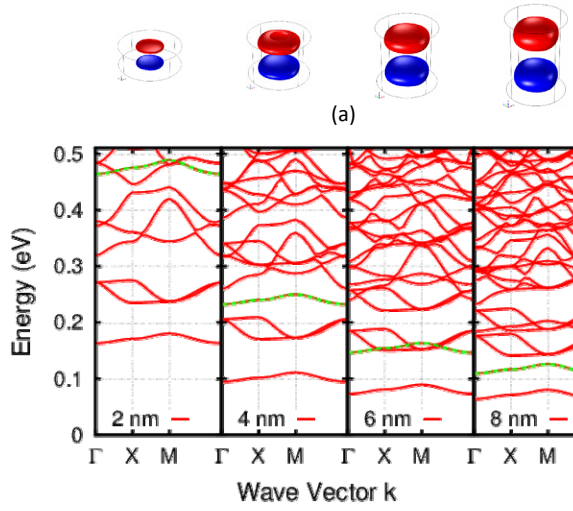

Fig. 5. (a) The first non-degenerate p-orbit along the z-direction with respect to QDs' thickness. (b) The band structures for Ge/Si disk-shaped QDs square superlattice with QD's radius of 3 nm, interdot space 0.3 nm, and varied thickness from 2 to 8 nm. The highlight band with p-orbit symmetry in the z-direction (green dash line) shows much dependence on the QDs' thickness.

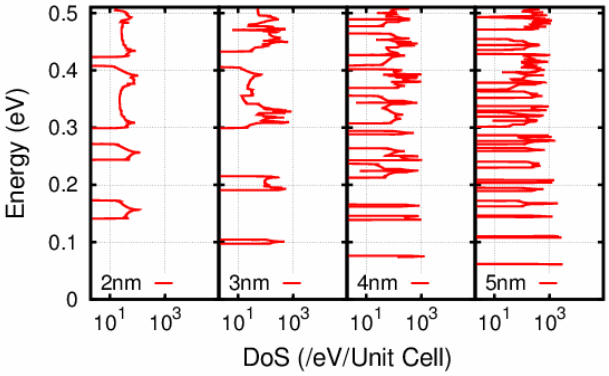

Fig. 6. The density of states for Ge/Si ellipsoid-shaped QDs square superlattice with QD's thickness of 6 nm, interdot space of 0.3 nm, and varied radius from 2 to 5 nm.

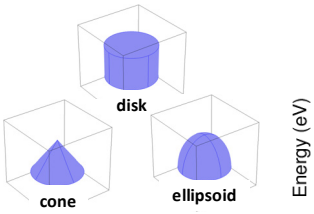

	Disk	Ellipsoid	Cone
r (nm)	3		
h (nm)	2 - 8	2 - 12	4 - 21

(a)

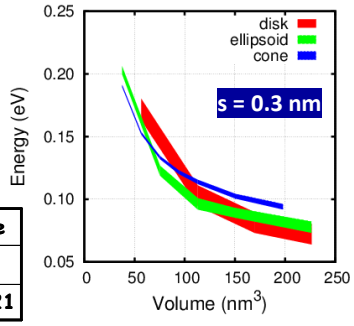

(b)

Fig. 7. (a) Three kinds of QDs shape used for comparison. (b) The energy level of ground band versus QDs volume for Ge/Si QDs square superlattice with different shapes of QDs. The width of stoke under the same volume represents the energy band width of ground state. The trend shows that the increasing in volume not only lead to the decreasing in energy but also enlarge the band width for three different shapes of QDs. Notably, the energy of disk-shaped QDs is more sensitive to volume among three shapes of QDs.